Supporting Online Material for

Interplay Between Changing Climate and Species' Ecology Drives Macroevolutionary Dynamics

Thomas H. G. Ezard,* Tracy Aze, Paul N. Pearson, Andy Purvis

*To whom correspondence should be addressed. E-mail: t.ezard@surrey.ac.uk

Published 15 April 2011, *Science* **332**, 349 (2011)
DOI: 10.1126/science.1203060

This PDF file includes:

Contents

1 Full Methods

1.1 Cenozoic macroperforate planktonic foraminifera

The complete phylogeny of Cenozoic macroperforate planktonic foraminifer species was developed from paleontological work that details the evolutionary relationships and temporal distributions of species identified morphologically and without molecular evidence (13). Under favorable conditions, the tests (shells) of dead individuals sink and accumulate continuously on the seabed forming an unparalleled resource for stratigraphic correlation (14), paleoclimatic reconstruction (15) and macroevolutionary research. Substantial temporal intergradation of morphospecies meant that we chose to perform all analyses on the phylogeny of evolutionary species' lineages (16) (hereafter, species) to minimize inflation of speciation and extinction rates caused by "pseudospeciation" and "pseudoextinction" (29). In $\sim 85\%$ of cases, persistent ancestry at the time of speciation (cladogenesis) could be assigned on the basis of morphological similarity (13). Each morphospecies was assigned to one of 19 groups delimited on test morphology and one of 6 delimited on inferred depth habitat (13).

1.2 Mathematical & Statistical Models

The support for particular statistical models was assessed using an information theoretic approach (25), selecting the model with most support among various combinations of diversity, climate, species' ecology as main effects and their two-way interactions (30).

1.2.1 Explanatory Variables

Models were constructed using data on all species that originated during the Cenozoic; two species (*Hedbergella holmdelensis* and *H. monmouthensis*) persisted through the end-Cretaceous mass extinction around 65 million years ago and were excluded from all analysis (31).

Because the planktonic foraminifera are distributed throughout the oceans, it is appropriate to compare their evolutionary patterns with the global climatic history of the Cenozoic era. Although climate change is complex and multifaceted, the oxygen isotopic composition (δ^{18}O) of deep sea carbonates provides a single time series recording direct, independent evidence for "trends, rhythms and aberrations" of Cenozoic climate history (15, 32). Isotopic signature shows substantial site-specificity (15), which we removed using a generalised additive model (GAM, 33) for use in our models. The δ^{18}O record (32) was regressed against age and the mean-centred, fitted values from the model were our paleoclimatic proxy. We set the upper limit on the number of knots, i.e. the "wiggliness" (33) of the curve, at 900 because the default settings (~ 9) capture the trends but not the aberrations and there were substantial improvements in fit (assessed by minimizing the general cross validation scores, 33) between intermediate (~ 90) and higher orders of magnitude, but not thereafter (Fig. S1). The climate at identical times was modeled as identical across all oceans on Earth; replicated time horizons were therefore removed to leave 14,572 values.

Many of the 19 morphogroups recognised in (13) consisted of very few species; we therefore pooled them into operational groups based on morphological innovations associated with exploitation of distinct ecological niches (presence/absence of keels, spines and

photo-symbionts; see main text). Of the 8 possible combinations of these binary morphological traits, six were observed across the 210-species phylogeny (group size ranged from 11 to 63). Depth habitat was similarly re-cast as a three-way categorical variable (mixed layer in tropical/subtropical oceans, thermocline and sub-thermocline; see main text) by assimilating the 10 species that inhabit upwelling zones or high latitudes into the mixed layer and sub-thermocline groups, respectively. The thermocline is the point in the water column where the temperature gradient is steepest.

1.2.2 Discrete-time models

The usual approach to circumvent the coarse temporal resolution of much of the fossil record is to amalgamate events in supposedly homogeneous periods of time and analyse diversification, origination and extinction rates within these discrete bins (8, 9). We used bin lengths of 1 myr for our discrete analysis to trade-off temporal replication against data completeness (Fig. S2): at a bin length of 1 million years, species have an 81% chance of being detected in the Neptune database (34, 35).

Clade growth ($ln(\frac{N_{t+1}}{N_t})$ where N_t denotes the number of species at time t) was detrended by taking first differences and then regressed against diversity at time t (ln-transformed), species ecology (proportions of species in the operational groups defined in §1.1.1 at time t), climate (mean [to investigate the direction of change] and range [to investigate the impact of climate variability within the bin] from time t to time $t+1$ of the fitted values from the GAM) and two-way interactions in a linear least-squares model. For model selection procedure, see §1.2.4. Interactions among species' ecology groups were not incorporated because bins early in the sequence (when there are very

few species in low numbers of operational groups) have significantly high influence on all model fits, suggesting over-parameterization (36). We present results with the first bin omitted because the number of species rose from 2 to 7 during this bin, which artificially increased variance explained in the models and produced unsatisfactory diagnostic plots (36). The ranking of most important models was unchanged between models using all data and those presented with this one outlier removed.

1.2.3 Continuous-time models

Functions for extinction and speciation were obtained independently, and then united in the continuous-time diversification model developed by Lotka (23) and extended by de Roos (22) to incorporate multiple types of individuals or, as here, species. Species' duration was regressed against ecology (as the binary groups defined in §1.1.1), overall diversity, climate and all two-way interactions using parametric survival regression models (24) to obtain parsimonious functions for speciation and extinction as detailed in §1.2.4. To control for the effect of diversity dependence and climate on clade growth, we assume that conditions early in a species' existence have long-lasting evolutionary consequences and remain constant as at the time of speciation; therefore climate variability was not incorporated in this analysis. In addition, we tested for a non-linear response by fitting our climate proxy additionally as a quadratic term. Minimum adequate models for speciation and extinction were obtained independently (Tables S2, S3) and then united in the continuous-time model. We used censoring when the last appearance date of a species was not an extinction or speciation date, as appropriate. For extinction functions, this meant censoring extant species and in the $\sim$15% of cases where neither descendant could

be identified unequivocally as the continuation of the ancestor; for speciation functions, it meant censoring extant species and extinct species that did not speciate.

We modeled time to speciation or extinction as Weibull random variables. A Weibull random variable a consists of two parameters – scale (λ) and shape (k) – and has probability diversity function:

$$f(a;k,\lambda) = \begin{cases} \frac{k}{\lambda}\left(\frac{a}{\lambda}\right)^{k-1} e^{-\left(\frac{a}{\lambda}\right)^{k}} & \text{if } a \geqslant 0 \\ 0 & \text{if } a < 0 \end{cases}$$

where λ is the scale parameter and k the shape parameter; both λ and k are strictly positive. If $k \neq 1$ then the hazard function, i.e. instantaneous risk of failure (24), changes with age (a). A biological interpretation of $k < 1$ is elevated extinction of young species (hazard decreases with age); if $k > 1$ then the converse is true and species are more likely to go extinct as they get older. A value of $k = 1$ indicates constant hazard; under this scenario the Weibull distribution simplifies to the exponential distribution. For our purposes, this case indicates that species have a constant probability of extinction throughout their existence, i.e. follow Van Valen's Law (1). Here, "hazard" represents the instantaneous probability of speciation or extinction of a species of age a. The Weibull hazard takes the form:

$$h(a;k,\lambda) = \frac{k}{\lambda}\left(\frac{a}{\lambda}\right)^{k-1}$$

According to the model (22, 23), the deterministic estimate of clade growth r is obtained by solving the following integral:

$$1 = \int_0^\infty e^{-r\alpha} b(\alpha) F(\alpha)\, d\alpha$$

$F(\alpha)$ in the Euler-Lotka equation is survival up to age α, which can be solved using hazard rates in the system of ordinary differential equations (ODEs) below. Following de Roos (22), let $L(a,r) = \int_0^a e^{-r\alpha} b(\alpha) F(\alpha)\, d\alpha$ and then solve the following system of ODEs under initial conditions of $S(0) = 1$ and $L(0,r) = 0$:

$$\frac{dS}{da} = -(m(a) + r)S(a) \qquad \frac{dL}{da} = b(a)S(a)$$

where $m(a)$ is the extinction hazard and $b(a)$ the speciation hazard modeled as Weibull random variables. $b(a)$ and $m(a)$ contained statistically significant effects of photosymbionts, keels and spines (Fig. S3, Table S3). Let $\mathbf{L}(A_m, r)$ be the matrix that relates the proportion of speciations in group i from an ancestral species in group j at a given age m:

$$\mathbf{L}(A_m, r) = \begin{bmatrix} L_{11}(A_m, r) & \cdots & L_{61}(A_m, r) \\ \vdots & \ddots & \vdots \\ L_{16}(A_m, r) & \cdots & L_{66}(A_m, r) \end{bmatrix}$$

The matrix is of rank 6 because that is the number of statistically-distinct groups observed; the main diagonal indicates species with the same morphology as their immediate ancestor while the off-diagonal elements relate species of a one type to ancestors of another type. Each element of $\mathbf{L}(A_m, r)$ is $L(a,r)$ as in the single-type case above for a particular combination of spines, keels and symbionts, scaled by the probability of having an ancestor of a particular group (we assumed this probability was constant and estimated it using observed mean transition rates). The system of ODEs outlined above is thus replaced by a multivariate version and, in this "multiple ecologies" case, r is the largest root (eigenvalue) of the multi-state dynamical system (22):

$$det(\mathbf{L}(A_m, r) - \mathbf{I}) = 0$$

where *det* indicates determinant and $\boldsymbol{I}$ the identity matrix. r was obtained numerically (37), using Newton-Raphson iteration procedures.

1.2.4 Model Selection

The statistical models with most support were obtained by fitting multiple combinations of explanatory variables (diversity, climate and ecology) as main effects and two-way interactions. We selected the most parsimonious model based on the corrected Akaike Information Criterion (AICc, 25). AICc provides a compromise between explanatory power and parameters used scaled by a correction factor for small sample size (as sample size increases, AICc converges on the "uncorrected" Akaike Information Criterion); if multiple models differed by < 2 values ($\Delta AICc < 2$) then all have "substantial" support and we prefer that with the fewest parameters as the most parsimonious (25). We also report model weights, which sum to 1 and can be interpreted as evidence weights, i.e. the probability that a particular model provides the optimal description of the data among the set of candidate models (25).

The improvement of fit in discrete models (Fig. 2) and the contributions to extinction and speciation hazards (Fig. 3) were calculated following a procedure for obtaining phenomenological time series models (30). The approach entails fitting combinations of explanatory variables and then comparing among them using some metric of explanatory power ($r^2, AICc, ...$). We calculated the difference in model fit between two candidate models using differences in AICc values because of the multi-parameter nature of the ecological groups. The difference between model fit of the minimum adequate (i.e., best) model and all other possibilities was calculated by removing each focal variable (including

interactions) in turn and comparing this new model with the minimum adequate model. The height of each bar in Fig. 3 is therefore the difference in AICc when each term is removed from the minimum adequate model, i.e., a measure of variance explained by that term only (30) and corrected for the degrees of freedom used by it (25).

The validation of the continuous-time model (Fig. S4) set the initial estimate of r for low diversities (N=10) at 0.3, and then iterated through increasing diversities using the preceding estimate of r for the initial estimate at subsequent diversity levels while holding the climate constant. Once r had been estimated for all diversity values in each climate state, climate was incremented (across the inter-quartile range) and the above procedure repeated until the lattices were filled.

1.2.5 Implementation and Software

All graphics were produced and analyses performed in the R environment for graphical and statistical computing (38) using the deSolve (37), mgcv (33), LASER (39), paleoPhylo (40) and survreg packages.

2 Supplementary Figures

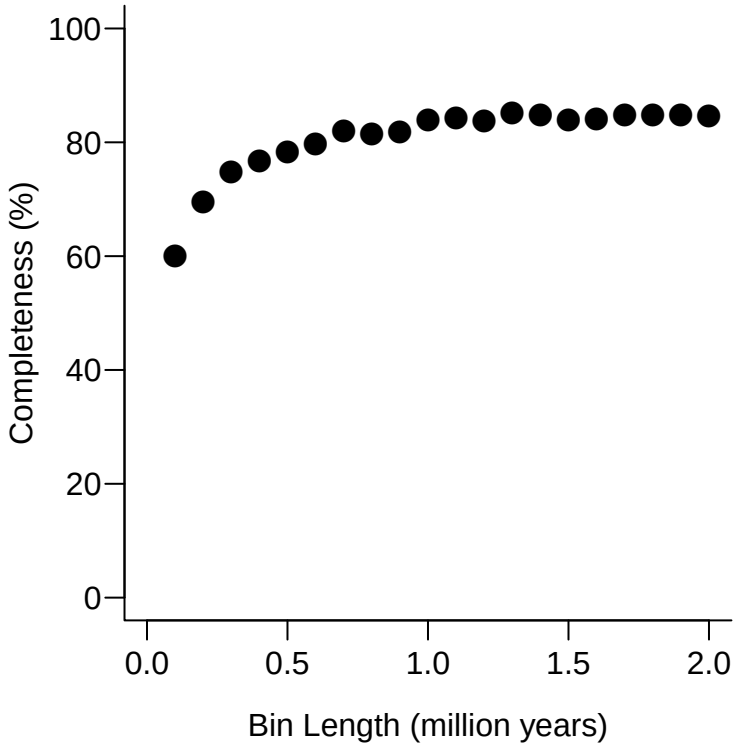

Figure S1. **At a bin length of 1 million years, Cenozoic macroperforate planktonic foraminifer species have a per-bin probability of 81% of being detected in the Neptune database (34, 35), suggesting that this species-level fossil record is at least as good as the best genus-level records among macro-invertebrate groups (17).** Data was downloaded from Neptune on 11-11-2010.

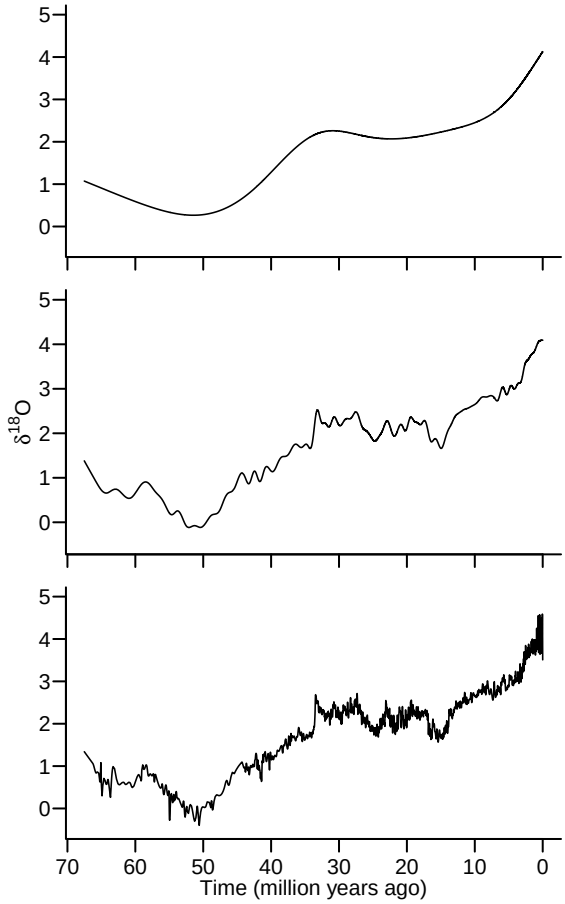

Figure S2. **Generalised additive models (33) were used to remove site specificity from the record of oxygen isotopic composition of deep sea (benthic) carbonates of the Cenozoic era (15, 32)**. We increased the number of knots k because the default settings (top, $k < 9$) captured the trends in climate but not the aberrations (note the Paleocene-Eocene Thermal Maximum around $\sim$ 55 million years ago, for example); the general cross validation scores for the curves were similar at intermediate $k < 90$ and high $k < 900$ levels, but inspection of diagnostic plots (residuals vs fitted values) were satisfactory only for the high level (note the Paleocene-Eocene Thermal Maximum around $\sim$ 55 million years ago, for example).

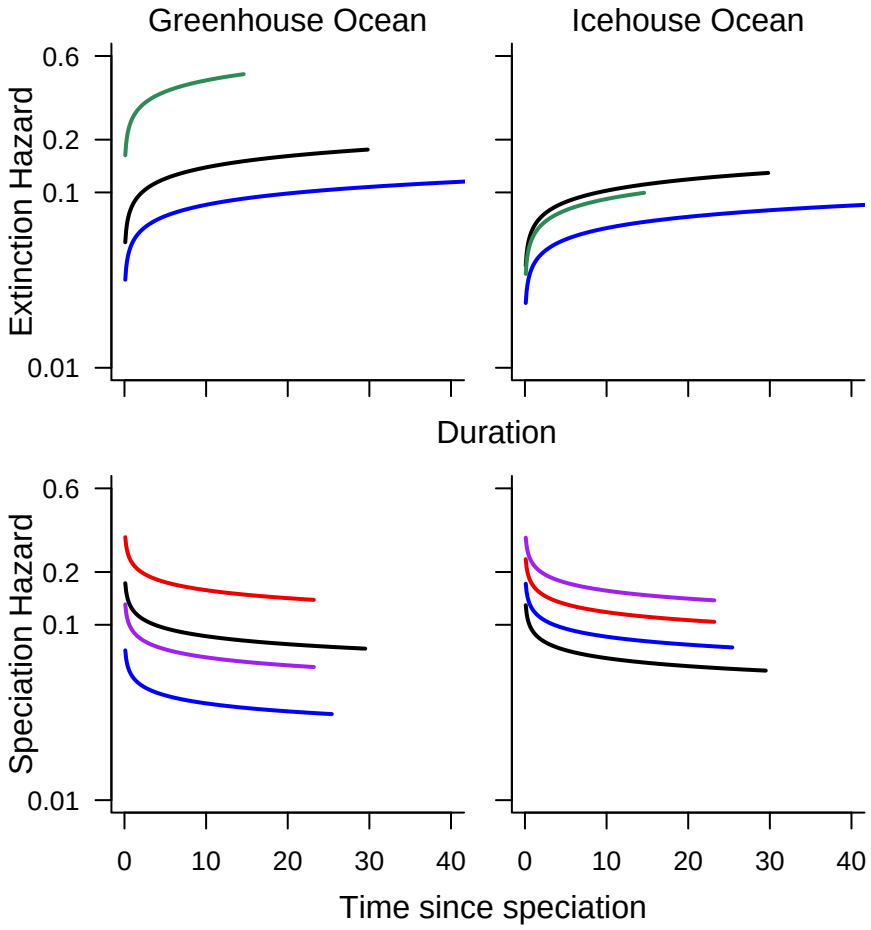

Figure S3. **Extinction and speciation hazards for statistically distinct ecological groups changed in rank between Greenhouse and Icehouse oceans**. Hazard functions give the instantaneous probability of the modeled event. Color codes are: blue - spinose; green - keeled; red - symbionts; purple - spinose and symbionts; and black all others. Curves are drawn (up to the maximum recorded duration for the focal group) at the 1st and 3rd climate quartiles to represent the greenhouse and icehouse oceans at overall mean diversity.

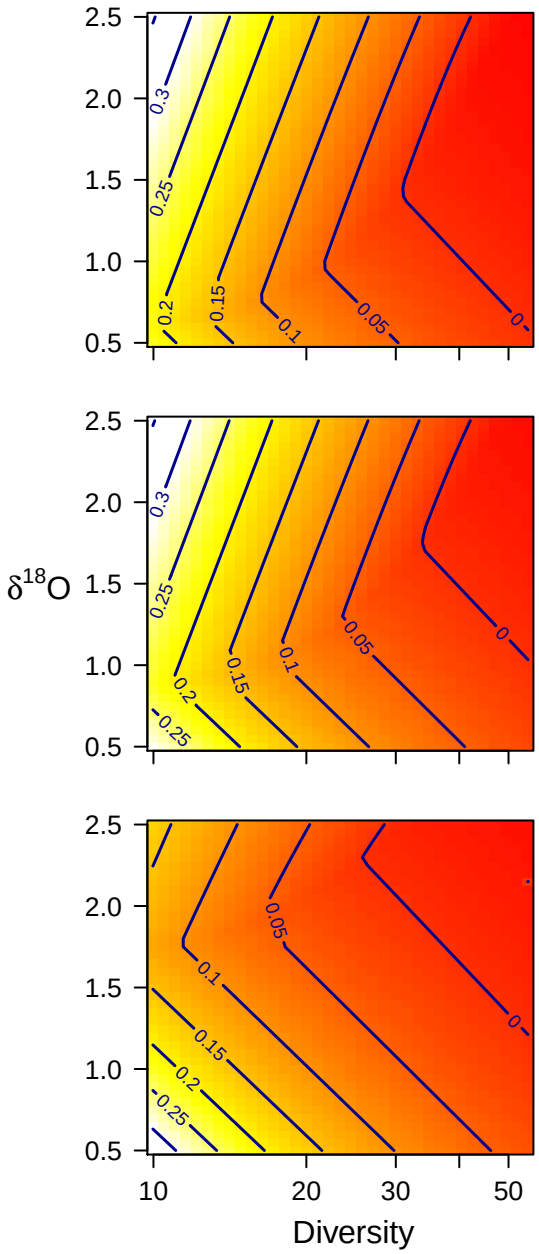

Figure S4. **The continuous-time model captured key features of the clade's macroevolutionary dynamics, including increased clade growth r at low and high values of our climate proxy and how different assemblages produce very different estimates of r even when all other parameters remain constant**. High δ^{18}O values reflect "greenhouse" oceans, whereas low δ^{18}O values are found in the more stratified oceans of today. The top panel is model estimates of r prior to the Eocene-Oligocene (E-O) transition; the middle panel is for the whole Cenozoic as reported in the main text; and the bottom panel for the post E-O assemblage.

3 Supplementary Tables

Model	r^2	Parameters	AICc	ΔAICc	Model Weight	Panel
MAM of D*C*E	0.6618	13	-247.2	0.0	0.9999	2f
D*E	0.4628	10	-227.3	19.9	0.0000	
D*C+E	0.4618	11	-224.2	23.0	0.0000	
D+E	0.3025	6	-221.5	25.7	0.0000	
D+C*E	0.5872	17	-220.5	26.7	0.0000	
Full	0.7255	23	-219.5	27.7	0.0000	
C*E	0.5450	16	-218.1	29.1	0.0000	2e
D+C+E	0.3090	8	-217.0	30.2	0.0000	
E	0.2060	5	-215.8	31.4	0.0000	2c
D*C	0.2598	7	-215.3	31.9	0.0000	2d
D	0.0459	2	-211.1	36.1	0.0000	2b
C+E	0.2093	7	-211.1	36.1	0.0000	
C	0.0533	4	-207.1	40.1	0.0000	2a
D+C	0.0468	4	-206.7	40.5	0.0000	

Table S1. **The best discrete-time models (ranked according to the corrected Akaike Information Criterion, AICc) featured interactions among diversity (D), climate (C) and species' ecology (E)**. Letter combinations indicate multiple driver models with * indicating multiplicative effects (up to second-order only) and + additive effects. Model weights can be interpreted as the probability that the model is the best of those fitted; r^2 is the adjusted value from a standard least-squares model (36) with sample size = (number of bins) - 1. "MAM" abbreviates "minimum adequate model" (see §1.2.4).

Group	Extinction	Speciation
Symbionts	$\zeta + \kappa D + \eta O$	$\zeta + \epsilon^{sy} + \kappa D + \eta O$
Spinose	$\zeta + \epsilon^{sp} + \kappa D + \eta O$	$\zeta + \epsilon^{sp} + \kappa D + (\eta + \eta^{sp})O$
Spinose & Symbionts	$\zeta + \epsilon^{sp} + \kappa D + \eta O$	$\zeta + \epsilon^{sp} + \epsilon^{sy} + \kappa D + (\eta + \eta^{sp})O$
Keeled	$\zeta + \epsilon^{kl} + \kappa D + \eta O$	$\zeta + \kappa D + \eta O$
Keeled & Symbionts	$\zeta + \epsilon^{kl} + \kappa D + \eta O$	$\zeta + \epsilon^{sy} + \kappa D + \eta O$
Other (Intercept)	$\zeta + \kappa D + \eta O$	$\zeta + \kappa D + \eta O$

Table S2. **Variables included to obtain the scale parameters in the Weibull hazard functions for the six statistically-distinct ecological groups observed**. Capital letters refer to non-constant variables (D and O are overall diversity and oxygen isotope ratios, respectively); greek letters are parameters estimated from parametric survival regression (24). ζ indicates intercept; κ diversity-dependence; ϵ intercept adjustments for keeled $^{(kl)}$, spinose $^{(sp)}$ and symbiont $^{(sy)}$ groups; η deep-sea (benthic) oxygen isotope ratios as the climate proxy; η^{sp} is the interaction between climate and spinose species.

	Extinction				Speciation			
Parameter	Coef.	S.E.	z	p	Coef.	S.E.	z	p
ζ	2.325	0.103	22.7	***	2.445	0.154	15.8	***
κ	-0.737	0.255	-2.88	**	0.785	0.180	4.37	***
η	0.155	0.082	1.90		-0.209	0.154	-1.36	
ϵ^{sp}	0.405	0.142	2.86	**	0.397	0.184	2.16	*
ϵ^{kl}	-0.393	0.241	-1.63					
ϵ^{sy}					-0.712	0.234	-3.036	**
η^{sp}					0.843	0.249	3.385	***
κ^{sp}	0.838	0.324	2.59	**				
η^{kl}	0.634	0.232	2.73	**				
$ln(k)$	-0.194	0.063	-3.08	**	0.164	0.059	2.77	**

Table S3. **Coefficients (Coef., with standard errors [S.E.], z-values and p-value codes) used in the extinction and speciation functions, obtained independently using parametric survival analysis with censoring (24)**. The parameter codes are: ζ intercept; κ diversity-dependence; ϵ intercept adjustments for keeled $^{(kl)}$, spinose $^{(sp)}$ and symbiont $^{(sy)}$ groups, respectively; η deep-sea (benthic) oxygen isotope ratios as the climate proxy; η^{sp} is the interaction between climate and spinose species; k is the shape parameter. The p-value codes are: *** $p < 0.001$; ** $p < 0.01$; * $p < 0.05$; $p > 0.05$; blank lines indicate that these terms were only significant for the other hazard. For model selection procedure, see §1.2.4. The corrected Akaike Information Criterion (AICc) scores were 1042.1 and 1153.4 for extinction and speciation, respectively.

Model	Parameters	AICc	ΔAICc	Model Weight
Birth-Death	2	85.61	0.00	0.288
Pure Birth	1	86.00	0.10	0.274
Exponential diversity-dependent speciation	2	86.91	1.30	0.151
Logistic diversity-dependent speciation	2	88.00	2.39	0.087
Exponentially declining speciation	3	87.58	2.43	0.086
Exponentially increasing extinction	3	87.62	2.46	0.084
Variable extinction and speciation	4	88.94	4.43	0.031

Table S4. **The best-supported, most-parsimonious model based on extant species only was a pure-birth model, highlighting the difficulty in inferring patterns of extinction based on extant species only**. Gamma (41) was -1.496 ($p > 0.05$ on a one-tailed test assuming complete taxon sampling), indicating a failure to reject the null hypothesis that speciation rates have decreased over time. Models were fitted using the LASER package (39); for model selection procedure, see §1.2.4.

References and Notes

1. L. Van Valen, A new evolutionary law. *Evol. Theory* **1**, 1 (1973).

2. M. J. Benton, The red queen and the court jester: Species diversity and the role of biotic and abiotic factors through time. *Science* **323**, 728 (2009). doi:10.1126/science.1157719 Medline

3. A. D. Barnosky, Distinguishing the effects of the red queen and court jester on miocene mammal evolution in the northern rocky mountains. *J. Vertebr. Paleontol.* **21**, 172 (2001). doi:10.1671/0272-4634(2001)021[0172:DTEOTR]2.0.CO;2

4. N. C. Stenseth, J. M. Smith, Coevolution in ecosystems: Red queen evolution or stasis? *Evolution* **38**, 870 (1984). doi:10.2307/2408397

5. C. Venditti, A. Meade, M. Pagel, Phylogenies reveal new interpretation of speciation and the red queen. *Nature* **463**, 349 (2010). doi:10.1038/nature08630 Medline

6. J. W. Valentine, Determinants of diversity in higher taxonomic categories. *Paleobiology* **6**, 444 (1980).

7. D. Jablonski, Species selection: Theory and data. *Annu. Rev. Ecol. Evol. Syst.* **39**, 501 (2008). doi:10.1146/annurev.ecolsys.39.110707.173510

8. J. Alroy, Colloquium paper: Dynamics of origination and extinction in the marine fossil record. *Proc. Natl. Acad. Sci. U.S.A.* **105** (suppl. 1), 11536 (2008). doi:10.1073/pnas.0802597105 Medline

9. J. Alroy, The shifting balance of diversity among major marine animal groups. *Science* **329**, 1191 (2010). doi:10.1126/science.1189910 Medline

10. M. Foote, Origination and extinction components of taxonomic diversity: Paleozoic and post-paleozoic dynamics. *Paleobiology* **26**, 578 (2000). doi:10.1666/0094-8373(2000)026<0578:OAECOT>2.0.CO;2

11. A. Purvis, Phylogenetic approaches to the study of extinction. *Annu. Rev. Ecol. Evol. Syst.* **39**, 301 (2008). doi:10.1146/annurev.ecolsys.063008.102010

12. T. B. Quental, C. R. Marshall, Diversity dynamics: Molecular phylogenies need the fossil record. *Trends Ecol. Evol.* **25**, 434 (2010). doi:10.1016/j.tree.2010.05.002 Medline

13. T. Aze *et al*., A phylogeny of Cenozoic planktonic foraminifera from fossil data. *Biol. Rev. Camb. Philos. Soc.* (2011); 10.1111/j.1469-185X.2011.00178.x.

14. W. A. Berggren, D. V. Kent, C. C. Swisher III, M.-P. Aubry, *A Revised Cenozoic Geochronology and Chronostratigraphy* (Society for Sedimentary Geology, Tulsa, OK, 1995).

15. J. Zachos, M. Pagani, L. Sloan, E. Thomas, K. Billups, Trends, rhythms, and aberrations in global climate 65 Ma to present. *Science* **292**, 686 (2001). doi:10.1126/science.1059412 Medline

16. G. G. Simpson, *Principles of Animal Taxonomy* (Columbia Univ. Press, New York, 1961).

17. M. Foote, J. J. Sepkoski Jr., Absolute measures of the completeness of the fossil record. *Nature* **398**, 415 (1999). doi:10.1038/18872 Medline

18. Materials and methods are available as supporting material on *Science* Online.

19. C. Hemleben, D. Mühlen, R. K. Olsson, W. A. Berggren, Surface texture and the first occurrence of spines in planktonic foraminifera from the early tertiary. *Geologische Jahrbuch A* **128**, 117 (1991).

20. R. D. Norris, Symbiosis as an evolutionary innovation in the radiation of paleocene planktic foraminifera. *Paleobiology* **22**, 461 (1996).

21. R. D. Norris, Extinction selectivity and ecology in planktonic foraminifera. *Palaeogeogr. Palaeoclimatol. Palaeoecol.* **95**, 1 (1992). doi:10.1016/0031-0182(92)90161-W

22. A. M. De Roos, Demographic analysis of continuous-time life-history models. *Ecol. Lett.* **11**, 1 (2008). doi:10.1111/j.1461-0248.2007.01121.x Medline

23. F. R. Sharpe, A. J. Lotka, A problem in age distribution. *Philos. Mag. Ser. 6* **21**, 435 (1911). doi:10.1080/14786440408637050

24. J. Kalbfleisch, R. L. Prentice, *The Statistical Analysis of Failure Time Data* (John Wiley, New York, 1980).

25. K. P. Burnham, D. R. Anderson, *Model Selection and Multimodel Inference. A Practical Information-Theoretical Approach* (Springer, New York, 2002).

26. S. Nee, Birth-death models in macroevolution. *Annu. Rev. Ecol. Evol. Syst.* **37**, 1 (2006). doi:10.1146/annurev.ecolsys.37.091305.110035

27. N. A. Doran, A. J. Arnold, W. C. Parker, F. W. Huffer, Is extinction age dependent? *Palaios* **21**, 571 (2006). doi:10.2110/palo.2006.p06-055r

28. A. B. Phillimore, T. D. Price, Density-dependent cladogenesis in birds. *PLoS Biol.* **6**, e71 (2008). doi:10.1371/journal.pbio.0060071 Medline

29. S. Stanley, S. Macroevolution, *Pattern and Process* (W. H. Freeman and Co., San Francisco, 1979).

30. T. Coulson *et al*., Estimating the functional form for the density dependence from life history data. *Ecology* **89**, 1661 (2008). doi:10.1890/07-1099.1 Medline

31. R. K. Olsson, C. Hemleben, W. A. Berggren, B. T. Huber, *Atlas of Paleocene Planktonic Foraminifera, No. 85 in Smithsonian Contributions to Paleobiology* (Smithsonian Institution Press, Washington, DC, 1999).

32. J. C. Zachos, G. R. Dickens, R. E. Zeebe, An early Cenozoic perspective on greenhouse warming and carbon-cycle dynamics. *Nature* **451**, 279 (2008). doi:10.1038/nature06588 Medline

33. S. N. Wood, *Generalized Additive Models: An Introduction with R, Texts in Statistical Science* (Chapman and Hall, Boca Raton, FL, 2006).

34. D. B. Lazarus, Neptune: a marine micropaleontology database. *Math. Geol.* **26**, 817 (1994). doi:10.1007/BF02083119

35. C. Spencer-Cervato, The Cenozoic deep sea microfossil record: Explorations of the DSDP/ODP sample set using the Neptune database. *Paleontol. Elect.* **2**, issue 2 (1999).

36. J. A. Fox, *An R and S-PLUS Companion to Applied Regression* (Sage Publications, Thousand Oaks, CA, 2002).

37. K. Soetaert, T. Petzoldt, R. W. Setzer, Solving differential equations in R: Package deSolve. *J. Stat. Software* **33**, issue 9 (2010).

38. R Development Core Team, *R: A Language and Environment for Statistical Computing* (R Foundation for Statistical Computing, Vienna, 2010).

39. D. L. Rabosky, LASER: A maximum likelihood toolkit for detecting temporal shifts in diversification rates from molecular phylogenies. *Evol. Bioinform. Online* **2**, 257 (2006).

40. T. H. G. Ezard, A. Purvis, paleoPhylo: Free software to draw paleobiological phylogenies. *Paleobiology* **35**, 460 (2009). doi:10.1666/0094-8373-35.3.460

41. O. G. Pybus, P. H. Harvey, Testing macro-evolutionary models using incomplete molecular phylogenies. *Proc. Biol. Sci.* **267**, 2267 (2000). doi:10.1098/rspb.2000.1278 Medline

Acknowledgments: We thank the Natural Environment Research Council (UK) for funding (grant NE/E015956/1 to A.P. and P.N.P.) and G. Mace, T. Barraclough, N. Bunnefeld, L.-M. Chevin, T. Coulson, L. McInnes, I. Owens, A. Phillimore, G. Thomas, and two anonymous reviewers for insightful comments that improved our work. The data we analyzed are deposited as online appendices to (*13*).